NUCLEAR INSTRUMENTS AND METHODS 135 (1976) 337–352; © NORTH-HOLLAND PUBLISHING CO.

A COMPILATION OF n–p AND n–C CROSS SECTIONS AND THEIR USE IN A MONTE CARLO PROGRAM TO CALCULATE THE NEUTRON DETECTION EFFICIENCY IN PLASTIC SCINTILLATOR IN THE ENERGY RANGE 1–300 MeV

A. DEL GUERRA

Istituto di Fisica dell'Università, Piazza Torricelli 2, I-56100 Pisa, Italy and
Istituto Nazionale di Fisica Nucleare, Sezione di Pisa, Via Livornese, S. Piero a Grado, I-56010 Pisa, Italy

Received 16 March 1976

A compilation of n–p and n–C cross sections is presented, with the purpose of giving useful information to compute the efficiency of neutron counters used in high energy physics experiments. Particular consideration is given to the cross sections for neutrons of kinetic energy up to 300 MeV. The results of a Monte Carlo program, in which these cross sections were used, are presented and compared with the experimental data on neutron counter efficiencies available in the literature. A very good agreement between experimental results and Monte Carlo predictions, on average much better than 10%, has been obtained.

1. Introduction

Several attempts have been made to compute the efficiency of organic scintillators for detecting high energy neutrons, between 1 and 200 MeV, using analytical[1,2]) and Monte Carlo methods[3,4]), taking into account both the neutron–hydrogen and the neutron–carbon interactions. However, the results of these calculations, when compared with the measured efficiencies of neutron detectors at present available in the literature [5–16]), have not always shown good agreement with the experimental data.

One of the crucial points of these calculations is the lack of available data for the n–C cross sections. Although the n–p and n–C total cross sections are well measured, the knowledge of the inelastic n–C cross section is rather poor. Moreover the relative contribution of the different inelastic channels to the total inelastic cross section is known only for the first few channels that open below 20 MeV and in an energy region that does not extend far beyond their threshold values The only accurate measurement at higher energies was made by Kellogg[17]) in a cloud chamber experiment, using a 90 MeV neutron beam. At that energy there are some one hundred inelastic channels open, each one having in the final state up to five ionizing particles, such as protons, deuterons, tritons, alpha particles and ionized nuclei. It is well known[18–21]) that the amount of light produced by a charged particle inside a scintillator is proportional to the ionization energy loss only for β-particles. The amount of light produced by a proton is reduced with respect to an electron of the same energy by the so-called p/β ratio; and as the atomic number of the particle increases so the light output produced decreases. Since this reduction factor also varies with the energy, it is clear that each n–C inelastic channel gives a contribution to the neutron detection efficiency in a scintillator that does not depend only on its cross section, but also strongly on the type of particles present in the final state. Such a dependence is of course more evident the higher the detection threshold.

It is therefore easy to understand why the computational methods, making very crude assumptions on the inelastic channel cross sections, do not often agree with the experimental efficiencies, in particular for counters having high threshold and for neutrons with a kinetic energy of the same order of magnitude as the threshold; on the other hand it is reasonable that most of the computations reproduce well the experimental data below 10 MeV, since the well-known n–p elastic scattering is the main contribution to the efficiency in that energy region.

Although numerous compilations of nucleon-nucleus cross section data are already present in the literature[22–25]), it is felt useful to present an updated list of the n–C cross section data in the energy range from 1 to 8000 MeV, with a particular emphasis on the inelastic channels. A list of the n–p cross sections is also given for the sake of completeness.

Not all of the total n–p and n–C experimental cross section measurements have been considered when there were enough data in the same energy region. Also some cross sections for the inelastic n–C channels have been deduced using plausible assumptions. Clearly the actual experimental picture does not allow us to disentangle all the inelastic channels. For the purpose of computation of neutron detection efficiencies in organic scintillators the only reasonable

TABLE 1
n–p total cross sections.

T_n (MeV)	σ_{np} (mb)	Ref.	T_n (MeV)	σ_{np} (MeV)	Ref.
10.6	780 ± 90	85	63.5	116.8 ± 2.6	38
12.5	690 ± 110	26	64.5 $^{+4.5}_{-5.5}$	126 ± 3	88
12.8	830 ± 90	85	66.1 ± 2.7	114.9 ± 2.5	38
13.5	694 ± 19	26	68 9 ± 3	109 6 ± 2.3	38
13.9	770 ± 40	67	72 ± 3.2	100 1 ± 2.3	38
14.0	700 ± 60	79	75.3 ± 3.5	100 3 ± 3.6	38
14.1 ± 0.05	689 ± 5	78	78.9 ± 3.8	94.7 ± 2.1	38
14.2	675 ± 20	73	82 8 ± 4	85.3 ± 1 9	38
14.8	610 ± 90	85	85	83 ± 4	41
15.0	660 ± 70	79	86.9 ± 4.3	82.1 ± 1.9	38
15.8 ± 0.33	537 ± 30	38	88	86.1 ± 2	62
16.13 ± 0.33	634 ± 34	38	88.5	84.5 ± 2	62
16.46 ± 0.34	580 ± 33	38	90	76 ± 1.7	61
16.5	680 ± 100	85	91.3 ± 4 6	77.7 ± 1.7	38
16.80 ± 0.35	597 ± 32	38	93.4	77 ± 5	45
17.15 ± 0.36	561 ± 29	38	95	73 ± 1.5	52
17.52 ± 0.37	544 ± 28	38	95	73.9 ± 3	90
17.90 ± 0.39	533 ± 27	38	96 ± 4.8	72.1 ± 1.6	38
18.1	550 ± 80	85	97 $^{+10}_{-6}$	73.9 ± 3	88
18 29 ± 0.40	517 ± 27	38	97.2	76 ± 3	45
18 69 ± 0.42	523 ± 28	38	97 ± 5	74 ± 10	70
19.11 ± 0.43	498 ± 40	38	101.1	80 ± 7	45
19.55 ± 0.44	522 ± 26	38	101 ± 5	71.5 ± 1.7	38
19.6	520 ± 90	85	106 ± 5.3	69.4 ± 1.6	38
19.655 ± 0.35	495 ± 3	49	106.8	59 ± 16	45
19.93	504 ± 10	48	115.5 ± 5.7	68 3 ± 2.1	38
20.0 ± 0.46	479 ± 24	38	117 ± 5	61.5 ± 8.6	70
20 46 ± 0.47	479 ± 22	38	126	56.9 ± 1.8	90
20.93 ± 0 48	449 ± 21	38	140 ± 5	48.5 ± 5 6	70
21.1	410 ± 90	85	153 ± 3	46 4 ± 1.2	89, 90
21.41 ± 0.5	447 ± 30	38	156 $^{+13}_{-7}$	46.4 ± 1.2	88
21.91 ± 0.51	420 ± 20	38	156 ± 5	50.5 ± 8 3	70
22.43 ± 0.52	408 ± 20	38	160	51.2 ± 2.6	53
22.96 ± 0.54	433 ± 19	38	169	49.2 ± 1.6	87
23.51 ± 0.57	397.7 ± 16	38	180 ± 7	44 ± 12	70
24.09 ± 0.59	393 ± 15	38	220	41 ± 4	53
24.69 ± 0.61	393.5 ± 15	38	220 ± 10	41.3 ± 3.5	70
25.0	390	83	247.47	42.80 ± 1.02	50
25.31 ± 0.63	362.9 ± 13.5	38	270	38 ± 1.5	51
25.94 ± 0.65	377.6 ± 12.7	38	278.69	38.63 ± 0 72	50
26.6 ± 0.68	345.7 ± 12.3	38	280	33 ± 3	58
27.29 ± 0.72	335.4 ± 11.5	38	311.12	37.32 ± 0.60	50
28.03 ± 0.76	321.5 ± 11.0	38	344.69	33.97 ± 0.57	50
28.80 ± 0.78	312.2 ± 12.5	38	379.30	34.09 ± 0.29	50
29.59 ± 0.80	309.1 ± 9.5	38	380	40 ± 4	55
30.40 ± 0.83	281.8 ± 8.8	38	380	34 ± 2	57
31.24 ± 0.86	286.4 ± 8.3	38	410	33.7 ± 1.3	75
32.12 ± 0.90	288.7 ± 7.4	38	414.87	33.90 ± 0.24	50
33.05 ± 0.96	276 ± 6.8	38	451.33	33.57 ± 0.24	50
34.03 ± 1.01	260.1 ± 7.2	38	488.61	34.16 ± 0.24	50
35.08 ± 1.07	245.8 ± 6.7	38	500	35 ± 2	57
36.20 ± 1.12	220 ± 9.9	38	526.65	34 94 ± 0.24	50
37.32 ± 1.15	226.8 ± 6.3	38	565.39	35 47 ± 0.23	50
38.0	223 ± 7.6	90	590	36.2	57

TABLE 1 (*continued*)

T_n (MeV)	σ_{np} (mb)	Ref
38.48 ± 1.21	223.5 ± 6.0	38
39 $^{+6}_{-5}$	223 ± 7.6	88
39.75 ± 1.29	219.1 ± 5.7	38
41.1 ± 1.38	204.6 ± 5.4	38
42.0	203 ± 7	63
42.0	170 ± 8.3	61
42.53 ± 1.45	196 ± 5.2	38
44.0 ± 1.50	189 ± 4.9	38
45.5 ± 1.6	187.3 ± 4.6	38
47.1 ± 1.7	170.3 ± 4	38
47.5	190 ± 10	62
48.8 ± 1.8	166.8 ± 4.1	38
50.6 ± 1.9	152.0 ± 3.8	38
52.5 ± 2.0	152.0 ± 3.6	38
54.5 ± 2.1	144.8 ± 3.3	38
56.6 ± 2.2	141.5 ± 3.1	38
58.8 ± 2.3	135.8 ± 2.9	38
61.1 ± 2.4	124.3 ± 2.8	38
63.0	126.0 ± 3	90

T_n (MeV)	σ_{np} (MeV)	Ref.
604.75	36.04 ± 0.23	50
630	37 ± 2	57
644.76	36.85 ± 0.22	50
685.31	37.60 ± 0.22	50
726.36	37.85 ± 0.22	50
767.89	37.98 ± 0.21	50
831.02	37.82 ± 0.16	50
916.55	38.12 ± 0.16	50
1003.47	38.21 ± 0.16	50
1091.60	38.85 ± 0.16	50
1180.78	39.35 ± 0.17	50
1290.83	39.99 ± 0.15	50
1400	42.4 ± 1.8	43
1447.03	40.50 ± 0.14	50
1630.25	40.67 ± 0.16	50
1851.27	40.75 ± 0.17	50
2151.64	40.76 ± 0.25	50
2470.42	40.83 ± 0.46	50

approach one can follow[1–4]) is to consider the inelastic cross section as if it were the sum of the contribution of only four channels, i.e. those channels for which data are available near threshold, and to extrapolate these cross sections to higher energies in a way consistent with both the total inelastic cross section and the scarce measurements of individual channels. In that sense this compilation is not intended to be a complete list of neutron cross sections but a useful guide to anybody who needs to compute neutron counter efficiencies.

2. n–p and n–C cross sections

As previously stated, the relevant cross sections describing the interaction of a neutron in an organic scintillator are the total n–p cross section (σ_{np}) and the total n–C cross section (σ_{nC}).

σ_{np} is very well measured and the experimental data between 10 and 2500 MeV are listed in table 1. For neutrons of kinetic energy (T_n) less than 50 MeV, the data are well parametrized as function of T_n expressed in MeV, by the following polynominal fit[97,98]):

$$\sigma_{np}(T_n) = 3\pi[1.206\,T_n + (-1.86+0.09415\,T_n + 0.0001307\,T_n^2)^2]^{-1} + \pi[1.206\,T_n + (0.4223+0.13\,T_n)^2]^{-1}.$$

The polynominal fit given by Clements and Winsberg[99]) for the n–p differential cross section, once integrated, gives less agreement with the experimental data and needs some corrections, as pointed out by Kurz[1]).

σ_{nC} is the sum of the elastic (σ_{el}) and inelastic (σ_{inel}) n–C cross section. Table 2 shows the experimental data for σ_{nC} and σ_{inel} at T_n greater than 15 MeV. At lower energies only a few points have been chosen, to show the trend of the cross section. Also shown in the table are the scarce experimental data on σ_{el}.

In fig. 1 the experimental data available for σ_{np}, σ_{nC} and σ_{inel} up to $T_n = 1000$ MeV are plotted; σ_{nC} has a behaviour common to all neutron–nucleus total cross sections, as pointed out by several authors[30,75,81,82]), after a rapid drop from a maximum near the threshold for nuclear reactions, it reaches a minimum at $T_n \approx 290$ MeV, which is the threshold for meson production, then increases to a broad maximum around 1.5 GeV, decreasing slowly thereafter[100]). A similar behaviour is also exhibited by σ_{inel} (see also ref. 25). The solid lines drawn on the figure are mostly obtained by means of computer minimization techniques[101]) applied to the data.

3. Breakdown of the n–C inelastic cross section

As described in section 1 a large number of inelastic channels opens up at T_n increases. We restrict our

TABLE 2

n–C total, inelastic and elastic cross sections.

T_n (MeV)	σ_{nC} (mb)	σ_{inel} (mb)	σ_{el} (mb)	Ref.
2.5	1570 ± 25^a			24
3.0	1750 ± 25^a			24
4.0	1850 ± 25^a			24
4.1			1800 ± 100	96
4.2			1800 ± 300	36
4.5	1700 ± 25^a			24
4.7	1500 ± 300			36
5.0	1200 ± 25^a			24
5.5	1125 ± 25^a			24
6.0	1100 ± 25^a			24
6.0			810 ± 80	60
6.2	1250 ± 25^a			24
6.3			1240 ± 120	60
6.4	1150 ± 25^a			24
7.0	800 ± 25^a	197.5 ± 15^a		24
7.0			520 ± 50	60
7.2	875 ± 25^a	220 ± 15^a		24
7.4	1750 ± 25^a	245 ± 15^a		24
7.6	1650 ± 25^a	270 ± 15^a		24
7.8	2200 ± 25^a	307.5 ± 15^a		24
8.0	1825 ± 25^a	350 ± 15^a		24
8.5	1050 ± 25^a	430 ± 15^a		24
9.0	1050 ± 25^a	520 ± 15^a		24
10.0	1160 ± 25^a	540 ± 15^a		24
10.2	1100 ± 10^a	542.5 ± 15^a		24
11.0	1520 ± 10^a	550 ± 15^a		24
11.5	1400 ± 10^a	552.5 ± 15^a		24
12.0	1500 ± 10^a	557.5 ± 15^a		24
12.5	1340 ± 10^a	560 ± 15^a		24
13.0	1420 ± 10^a	565 ± 15^a		24
14.0	1280 ± 10^a	572.5 ± 14^a		24
14.0			775 ± 40	91
14.1			805	84
14.5			770 ± 40	42
14.6			790 ± 50	74
15.0	1440 ± 10^a	582.5 ± 15^a		24
15.80 ± 0.33	1460 ± 32			38
16.13	1480 ± 32			38
16.46	1450 ± 31			38
16.6		236 ± 21^b		6
16.80	1450 ± 31			38
17.15 ± 0.36	1470 ± 31			38
17.52 ± 0.37	1390 ± 30			38
17.90 ± 0.39	1520 ± 30			38
18.29 ± 0.40	1470 ± 30			38
18.69 ± 0.42	1480 ± 30			38
19.11 ± 0.43	1450 ± 29			38
19.3		357 ± 26^b		6
19.55 ± 0.44	1480 ± 45			38
20 ± 0.46	1450 ± 28			38
20.46 ± 0.47	1500 ± 28			38
20.93 ± 0.48	1460 ± 27			38
21.0		490 ± 40		69
21.41 ± 0.50	1410 ± 25			38

TABLE 2 (*continued*)

T_n (MeV)	σ_{nC} (mb)	σ_{inel} (mb)	σ_{el} (mb)	Ref.
21.9		354 ±27[b]		6
21.9 ± 0.51	1420 ± 25			38
22.43 ± 0.52	1396 ± 23			38
22.96 ± 0.54	1439 ± 22			38
23.51 ± 0.57	1367 ± 22			38
24 09 ± 0.59	1375 ± 21			38
24.6		324 ±24[b]		6
24.63	1389 6 ± 1.7			39
24.69 ± 0.61	1393 ± 21			38
25.31 ± 0.63	1340 ± 20			38
25.5		440 ±40		69
25 94 ± 0.65	1335 ± 20			38
26.6 ± 0 68	1349 ± 19			38
27.27 ± 0.72	1315 ± 18			38
27.4		378 ±29[b]		6
28.03 ± 0.76	1298 ± 18			38
28 8 ± 0.78	1291 ± 17			38
29.2		450 ±40		69
29.25	1311.2 ± 1.7			39
29.59 ± 0.8	1358 ± 16			38
30.40 ± 0.83	1250 ± 16			38
31 24 ± 0.86	1237 ± 15			38
31.6		303 ±22[b]		6
32.12 ± 0.90	1220 ± 15			38
33.05 ± 0.96	1231 ± 14			38
34.03 ± 1.01	1203 ± 20			38
34 4		428 ±34[b]		6
35 08 ± 1.07	1180 ± 14			38
36 2 ± 1 12	1121 ± 13			38
36.34	1179 ± 1.4			39
37.32 ± 1 15	1143 ± 13			38
37.6		307 ±23[b]		6
38.48 ± 1 21	1123 ± 12			38
39.56	1130.7 ± 1.2			39
39.75 ± 1 25	1096 ± 12			38
41.1 ± 1.38	1081 ± 11			38
41.2		338 ±25[b]		6
42 53 ± 1.45	1068 ± 11			38
44 ± 1.5	1052 ± 11			38
44.6		295 ±25[b]		6
45.5 ± 1 6	1012 ± 10			38
46.18	1012.7 ± 1.4			39
47.10 ± 1 7	967 ± 9			38
47.5 ± 12	984 ± 30			62
47.9		315 ±27[b]		6
48.80 ± 1.80	969 ± 9			38
50 60 ± 1.90	930 ± 9			38
50 9		309 ±35[b]		6
52 ± 1 5	892 ± 22			90
52.5 ± 2.0	912 ± 9			38
52.8		280 ±31[b]		6
54.5 ± 2.1	879 ± 9			38
54.8		301 ±33[b]		6
55 ± 2		278 ±54		95
56 6 ± 2.2	844 ± 8			38
56 9		291 ±32[b]		6

TABLE 2 (*continued*)

T_n (MeV)	σ_{nC} (mb)	σ_{inel} (mb)	σ_{el} (mb)	Ref
58.8 ± 2.3	808 ± 8			38
58.9		327 ± 36^{b}		6
60 ± 1.5	789 ± 12			90
61 ± 0.5	674 ± 62			44, 45
61 ± 4.5		200 ± 13		72
61.1		226 ± 24^{b}		6
61.1 ± 2.4	782 ± 7			38
63 ± 1.6	784 ± 5			90
63.5 ± 2.5	775 ± 7			38
63.5		259 ± 27^{b}		6
66.1 ± 1.0	671 ± 42			44, 45
66.2		231 ± 24^{b}		6
66.2 ± 2.7	740 ± 7			38
68.9 ± 3.0	698 ± 9			38
69.1		269 ± 28^{b}		6
71.2 ± 0.5	601 ± 41			44, 45
72.0 ± 3.2	666 ± 6			38
72.3		232 ± 24^{b}		6
75.3 ± 3.5	654 ± 6			38
76.1		284 ± 29^{b}		6
76.7 ± 0.5	614 ± 31			44, 45
78	590 ± 15			68
78.9 ± 3.8	617 ± 6			38
80.0		261 ± 27^{b}		6
81 ± 0.2		202 ± 20		95
81.2 ± 1.0	585 ± 17			44, 45
82.8 ± 4.0	582 ± 6			38
83.5		259 ± 26^{b}		6
84 ± 1.5	571 ± 6			90
85	545 ± 10			68
85 ± 28	550 ± 11			41
85.5 ± 0.5	602 ± 19			44, 45
86.9 ± 4.3	555 ± 6			38
87.5		245 ± 25^{b}		6
88	530 ± 10			68
88 ± 2	560 ± 8			62
88.2 ± 1	547 ± 11			71
90 ± 25			250 ± 60^{c}	18
91.0		206 ± 25^{b}		6
91.3 ± 4.6	535 ± 6			38
92.3 ± 7	520 ± 80			44, 45
93.4 ± 0.5	518 ± 6			44, 45
95 ± 1.5	508 ± 5			88, 89
95 ± 26	498 ± 3	223 ± 7	173 ± 8	52
96.0 ± 4.8	509 ± 6			38
96.0		206 ± 21^{b}		6
97.0 ± 5	500 ± 12			70
97.2 ± 1.0	494 ± 4			44, 45
98.1 ± 1	490 ± 10			71
99.4 ± 4	518 ± 4			44, 45
100	470 ± 10			68
101 ± 5	472 ± 6			38
101.1 ± 0.5	466 ± 7			44, 45
101.5		193 ± 19^{b}		6
105 ± 3		234 ± 8		95
106 ± 5.3	456 ± 5			38

TABLE 2 (*continued*)

T_n (MeV)	σ_{nC} (mb)	σ_{inel} (mb)	σ_{el} (mb)	Ref
106.8 ± 2	508 ± 14			44, 45
107.0		232 ± 25[b]		6
110 ± 1	439 ± 9			71
111	437 ± 8			40
111.5 ± 5.7	435 ± 7			38
113.5		208 ± 24[b]		6
114	420 ± 15			68
117 ± 2	408 ± 4			90
117 ± 5	392 ± 6			70
117.5 ± 6.0	405 ± 12			38
119.6 ± 1	403 ± 8			71
120.0		188 ± 23[b]		6
126 ± 2	390 ± 3			88
129.4 ± 1	375 ± 8			71
131	365 ± 15			68
136			159 ± 11[c]	94
136			144 ± 11[c]	94
139 ± 3	355 ± 3			90
140 ± 5	349 ± 4			70
140 ± 4		221 ± 9.5		95
140.9 ± 1	346 ± 7			71
150.9 ± 1	341 ± 7			71
153 ± 3	330 ± 3			88, 89
155	270 ± 20			68
156 ± 5	325 ± 10			70
160 ± 30	296 ± 6			53
169 ± 4	323 ± 3			87
180 ± 7	311 ± 9			70
190 ± 40	291 ± 9			53
220 ± 10	296 ± 3			70
220 ± 45	285 ± 60			53
270 ± 60	288 ± 3	145 ± 6	143 ± 7	51
280 ± 45	279 ± 4			58
300		203 ± 33		33
351.5 $^{+1.5}_{-1.0}$	285.3 ± 1.6	200.8 ± 4.7	≥84.5 ± 4.5	29, 30, 31
379	299 ± 8	268 ± 45	31 ± 45.7	81, 82
380 ± 50	286 ± 2			57
410 ± 20	297 ± 3			75
414	287 ± 8	261 ± 38	26 ± 38.83	81, 82
451	317 ± 8	242 ± 32	75 ± 32.98	81, 82
488	317 ± 8	233 ± 28	84 ± 29.12	81, 82
500 ± 70	306 ± 2			57
545	333 ± 6	210 ± 18	123 ± 18.97	81, 82
590 ± 80	319 ± 2			56, 57
624	328 ± 6	248 ± 15	80 ± 16.15	81, 82
630	342 ± 1.5			64
630 ± 85	338 ± 5			57
705	350 ± 6	260 ± 13	90 ± 14.36	81, 82
765 ± 30	342.1 ± 3.7	198 ± 18	144 ± 19	37
788	353 ± 6	242 ± 11	111 ± 12.5	81, 82
873	351 ± 7	259 ± 10	92 ± 12.5	81, 82
959	358 ± 7	261 ± 10	97 ± 12.2	81, 82
1069	352 ± 7	268 ± 9	84 ± 11.4	81, 82
1202	380 ± 7	255 ± 8	125 ± 10.6	81, 82
1361	314 ± 8	258 ± 6	106 ± 9.2	81, 82
1400 ± 200	378 ± 10	201 ± 13	177 ± 16	43

TABLE 2 (*continued*)

T_n (MeV)	σ_{nC} (mb)	σ_{inel} (mb)	σ_{el} (mb)	Ref.
1545	363 ± 8	268 ± 6	95 ± 10	81, 82
1731	408 ± 12	251 ± 8	157 ± 14.4	81, 82
5000 ±400	319 ± 20	235 ±16	84 ± 26	32
8300	345 ± 15	218 ± 8	127 ± 17	76

---

[a] Taken from the "recommended line" in ref. 24.

[b] This cross section may be as much as 30% lower for $T_n < 30$ MeV, and has to be considered as the lower limit to the true σ_{inel} for higher T_n.

[c] Based on optical theorem.

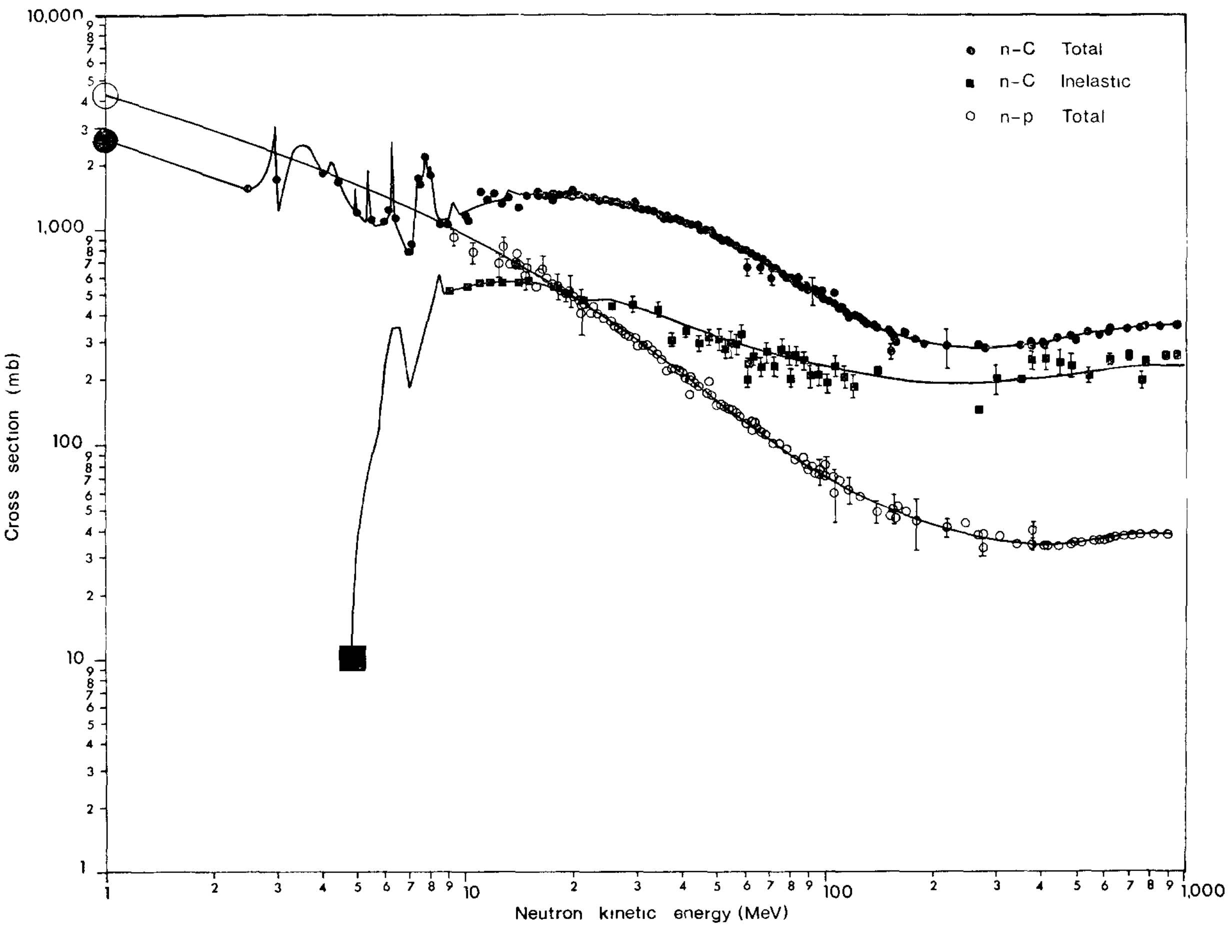

Fig. 1. n–C total, n–C inelastic and n–p total cross sections data. The full lines show the cross sections used in the Monte Carlo program.

discussion to the region up to 300 MeV, for beyond that value the neutron detection efficiencies depend mostly upon the total n–C inelastic cross section, and the knowledge of the different branching ratios is much less relevant to the computation.

TABLE 3

n–C inelastic reactions and parameters.

Channel	Reaction	Q (MeV)	Threshold (MeV)
$(n,n'\gamma)$	$n + {}^{12}C \rightarrow n' + {}^{12}C + \gamma$	−4.43	4.7
(n,α)	$n + {}^{12}C \rightarrow \alpha + {}^{9}Be$	−5.709	6.2
$(n,n'3\alpha)$	$n + {}^{12}C \rightarrow n' + 3\alpha$	−7.281	7.9
(n,p)[a]	$n + {}^{12}C \rightarrow p + {}^{12}B$	−12.593	13.6

[a] This channel is usually taken to include (n,d) channels that opens at 14.9 MeV, there being no data available for this latter channel around its threshold region or above

TABLE 4

$(n,n'\gamma)$ cross sections.

T_n (MeV)	$\sigma_{(n,n'\gamma)}$ (mb)	Ref
6.0	240 ± 20[a]	60
6.3	350 ± 20[a]	60
6.58	348 ± 57	47
7.0	170 ± 20[a]	60
8.5 ± 0.5	445 ± 25[b]	1
9.0 ± 0.5	345 ± 25[b]	1
14.0	225 ± 8[c]	77
14	261 ± 39	34, 35, 54
14	220 ± 30[a]	28, 31
14.1	~300	92
14.1	200	84
14.7	206 ± 6[c]	77
15.2	210 ± 7[c]	77
15.6	196 ± 6[c]	77
16.2	179 ± 5[c]	77
16.7	157 ± 4[c]	77
17.4	137 ± 6[c]	77
17.8	144 ± 4[c]	77
17.9	130 ± 6[c]	77
18.4	134 ± 6[c]	77
18.9	127 ± 3[c]	77
19.4	127 ± 4[c]	77
96	13.75 ± 2.5[d]	86
185	7.7 ± 1.5[c]	93

[a] May be underestimated, being the cross section for excitation of the 4.43 MeV level (see also ref 105).

[b] Cross section and error estimated from the figure in ref. 1.

[c] Taken from p–C scattering.

[d] Estimated as 5% of the n–C elastic cross section.

Because of lack of experimental data, all analytical and Monte Carlo computations of neutron counter efficiencies[1-4]) treat the total inelastic cross section as the sum of the contribution of only four channels, as mentioned previously. These are listed in table 3, according to their increasing threshold.

Although the (n, 2n) channel, whose threshold is 20.3 MeV, is known around its threshold region and above, this channel is not usually[1-4]) taken into account, because it does not contribute directly to the efficiency and its cross section is still less than 10% of the inelastic cross section at 90 MeV[17]); therefore no experimental data are presented, but some can be found elsewhere[23,24,104]).

In tables 4 and 5 are listed the experimental data for $\sigma_{(n,n'\gamma)}$, $\sigma_{(n,\alpha)}$, $\sigma_{(n,n'3\alpha)}$ and $\sigma_{(n,p)}$, which are also plotted in fig. 2, together with the experimental data for σ_{inel}. The full lines on the figure were drawn on the basis of reasonable assumptions, using the following procedure:

1) First of all $\sigma_{(n,n'\gamma)}$ was isolated, whose experimental points well exhibit the sharp resonances expected in the yield of 4.43 MeV γ-rays[105]). The broad resonance around $T_n = 14$ MeV takes into account the excitation of carbon levels from 4.4 to 9.6 MeV with decay to the ground state through emission of 4.43 γ-rays directly or through

TABLE 5

(n,α), $(n,n'3\alpha)$, (n,p) cross sections.

T_n (MeV)	$\sigma_{(n,\alpha)}$ (mb)	$\sigma_{(n,n'3\alpha)}$ (mb)	$\sigma_{(n,p)}$ (mb)	Ref.
7.8	46 ± 10[a]			46
8.0	73 ± 10[a]			46
8.5	34 ± 10[a]			46
9.0	30 ± 10[a]			46
12.9		190 ± 50		59
14.0	62 ± 15			27
14.1	76 ± 11			65
14.1		230 ± 50		59
14.92			1.93 ± 0.25	66
15.08			5.69 ± 0.68	66
15.5		316 ± 73		59
16.59			19.56 ± 2.74	66
17.51			29.09 ± 4.36	66
18.8		283 ± 59		59
90 ± 30	4 ± 2	39 ± 10[b]	182 ± 27[c]	17

[a] Averaged over several experimental points

[b] Estimated from ref. 17 as sum of all the $(n,n'2\alpha)$ and $(n,n'3\alpha)$ channels.

[c] Estimated as the remaining contribution to the inelastic cross section, see also text.

an intermediate unstable ^{8}Be–α state[80,106]). Beyond 14 MeV the data available for p scattering on carbon[77,93]) have been used, since the n–C and p–C elastic and quasi-elastic scattering are essentially identical above that energy[28,74]); above 20 MeV, $\sigma_{(n,n'\gamma)}$ has been smoothed down through the higher energy experimental values.

2) The $\sigma_{(n,n'\gamma)}$ so obtained was then subtracted from σ_{inel} and the remaining $\sigma_{(n,\alpha)}$ was deduced in the region up to 20 MeV, where $\sigma_{(n,n'3\alpha)}$ and $\sigma_{(n,p)}$ are known; its value agrees with the experimental values[65,107 108]) and with experimental indications obtained by measuring neutron counter efficiencies[4,14]). $\sigma_{(n,\alpha)}$ was then smoothed down using the measured experimental value[17]) at 90 MeV, as a normalization point.

3) The two remaining channels were then isolated over the full energy region. The data of Kellogg[17]) were used to normalize the cross section values at 90 MeV in the following way: $\sigma_{(n,n'3\alpha)}$ was assumed to be equal to the sum of the contributions of all the channels with 2α or 3α in the final state, and $\sigma_{(n,p)}$ was assumed to take the remaining part of σ_{inel}

4) The sum of the four inelastic channels considered was made to be equal to the total inelastic cross section experimental data, within the errors, over the full energy range.

The validity of this procedure was then checked by using these cross sections in a Monte Carlo program[109]) whose results were compared with the available experimental data on neutron counter efficiencies, the agreement between experimental and Monte Carlo efficiency values was found to be quite remarkable, as illustrated in section 4

4. Monte Carlo program results

The Monte Carlo program was originally written[109]) in order to extend to different illumination conditions and to higher energies the set of efficiency measurements of a modular neutron detector in the energy range 15–120 MeV[110 111]) The main features of the

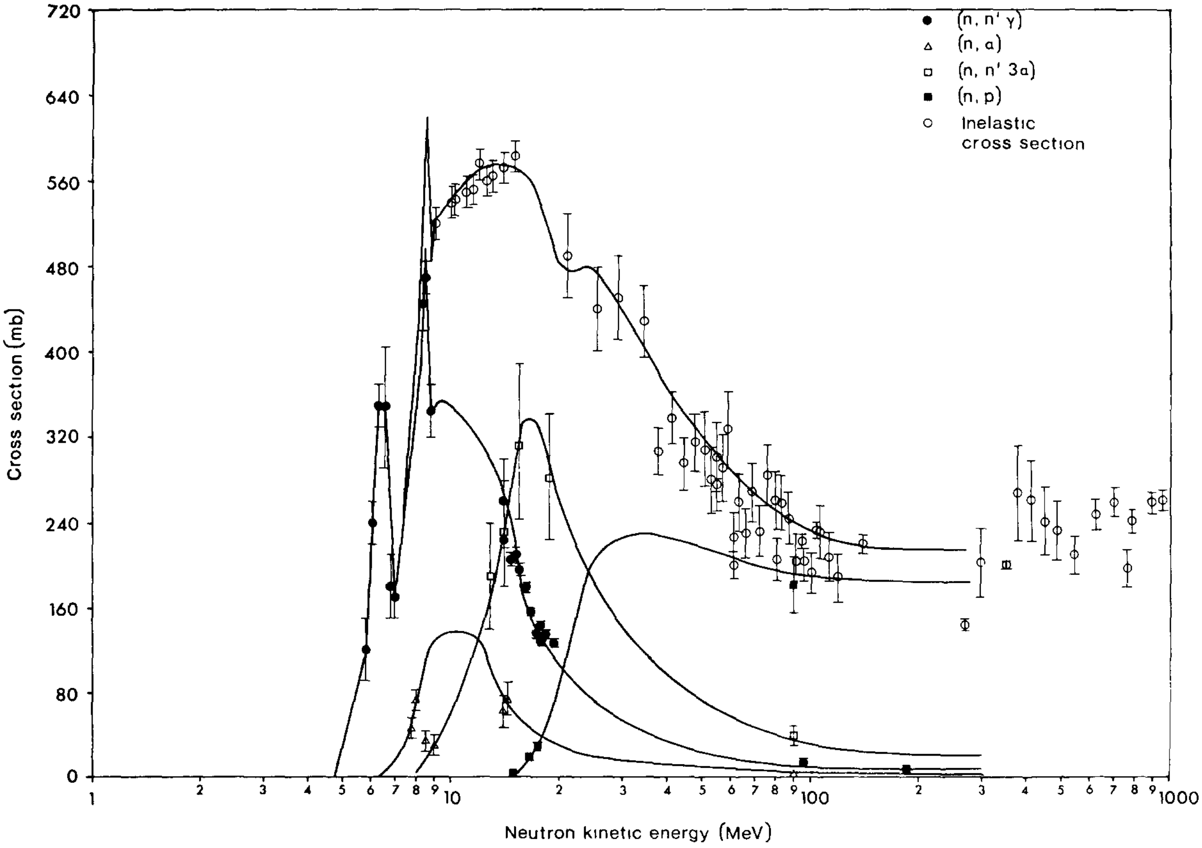

Fig. 2. $\sigma_{(n,n',\gamma)}$, $\sigma_{(n,\alpha)}$, $\sigma_{(n,n'3\alpha)}$, $\sigma_{(n,p)}$ and n–C inelastic cross sections data. The full lines show the cross sections used in the Monte Carlo program,

Monte Carlo and its comparison with the measured efficiency of such a counter have been already presented in a previous paper[111]). A comparison of the Monte Carlo prediction with a second set of efficiency measurements of a large neutron detector of the same modularity[112,113]) at higher energy, up to $\sim$500 MeV, may be found in ref 114 In this section the Monte Carlo results are compared with most of the available data on neutron counter efficiencies[5,7–10,12–16]), which have been measured at various threshold values from 0.2 to 37 MeV eq el en , for neutron kinetic energy (T_n) up to 200 MeV Some comments are also made in comparison with similar predictions obtainable by means of other computational methods[1–3])

When calculating neutron counter efficiencies, one must be very careful in reproducing the conditions relevant to each experiment, such as the correct geometry of the counter, the threshold setting and the energy uncertainty of the incident neutrons. The presence of shielding in front of the detector, the overall light output response of the counter and the pulse shaping must be also carefully reproduced, as they play an important role for a correct computation, especially in the energy region immediately above the threshold, where the efficiency increases rapidly from zero and depends very strongly on energy Other authors have already pointed out the importance of finite size effects[115]) and of the light attenuation effects[116]) in the calculation of neutron detector efficiencies In our computation we have tried to take into account all these parameters, although sometimes it was somewhat difficult to extract from the papers all the information needed to make a correct simulation

Figs 3a–d show the experimental efficiencies together with the Monte Carlo predictions for four counters of thickness ranging between 150 and 305 mm. The data of Wiegand et al [5]) (fig. 3a) are very well reproduced

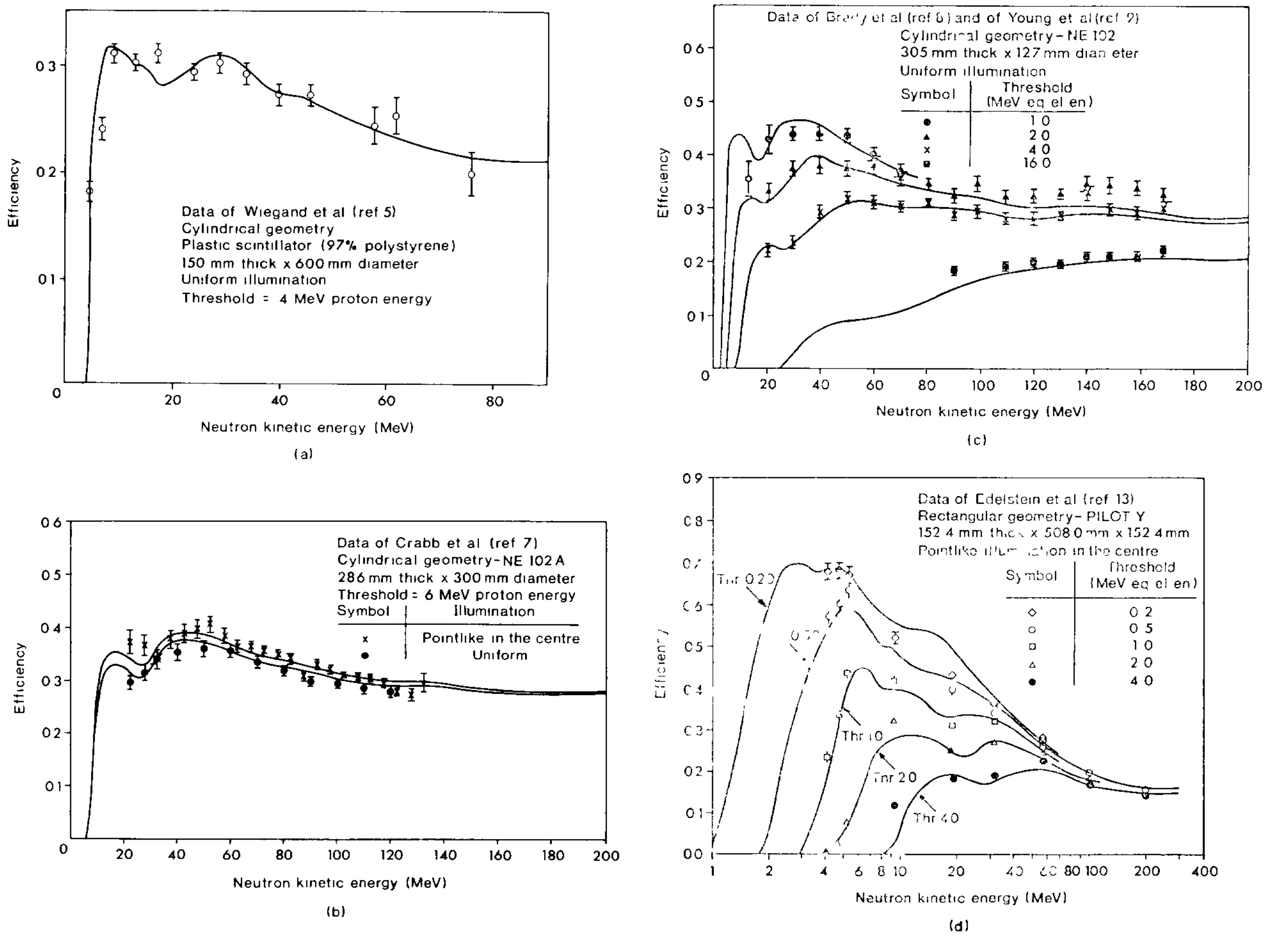

(a)

(b)

(c)

(d)

Fig 3 Comparison of efficiency measurements with the Monte Carlo predictions for neutron counters between 150 and 305 mm thick (a) Wiegand et al [5]), (b) Crabb et al [7]), (c) Brady et al [8]) and Young et al [9]), (d) Edelstein et al [13])

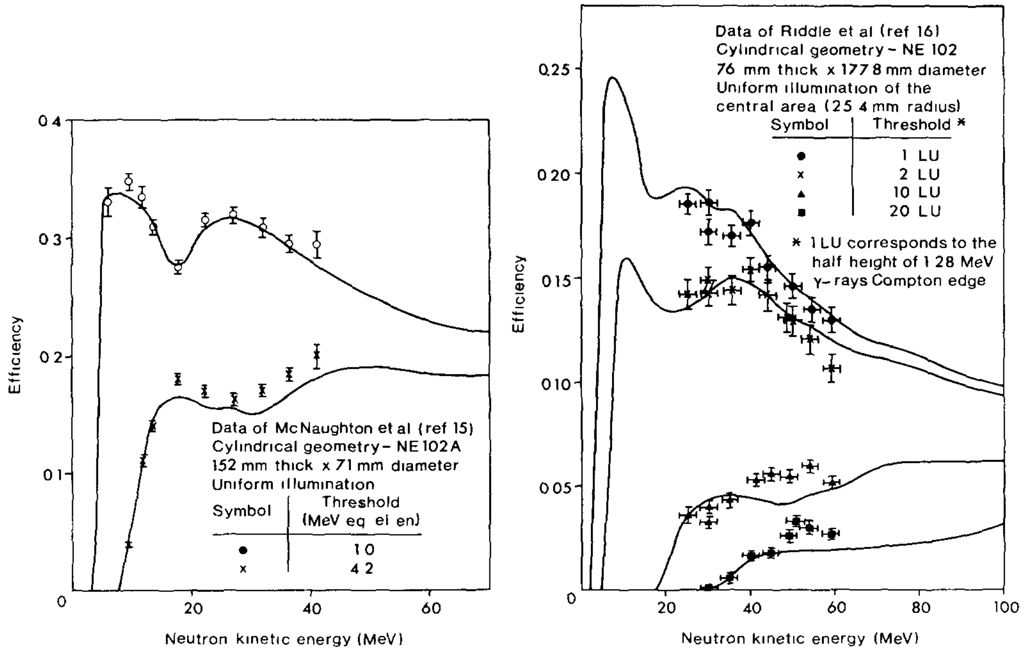

(a) (b)

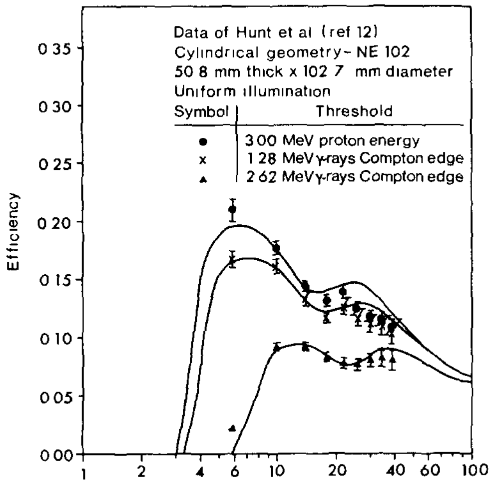

(c)

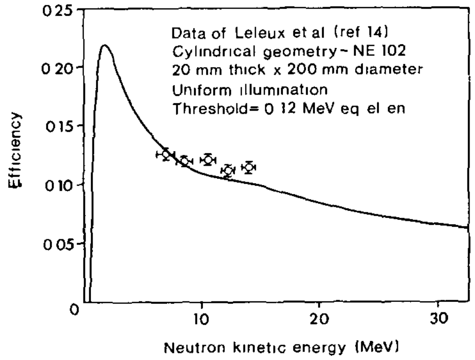

(d)

over the full energy range; so are the data of Crabb et al.[7]) (fig. 3b) for both the pointilike and the uniform illumination conditions, which guaranteed the correct treatment of edge effects. The data of Brady et al.[8]) and Young et al.[9]) are also well simulated by the Monte Carlo (fig. 3c), when ~10% lower threshold was used. For $100 < T_n < 170$ MeV at a threshold of 2.0 MeV eq el. en, the data are as much as 10% higher than the Monte Carlo prediction; on the other hand such a discrepancy is not present at a threshold twice as big, nor would one expect such a dependence of the efficiency on threshold in that energy range. The comparison with the data of Edelstein et al.[13]) (fig. 3d) is also very satisfactory, although a small disagreement of ~5–10% may be noticed for a few points.

The experimental efficiencies of counters between 20 and 150 mm thick are shown in figs. 4a–d, together with the Monte Carlo predictions. The agreement is striking for the data of McNaughton et al.[15]) (fig. 4a) at the threshold of 1.0 MeV eq. el. en.; at the higher threshold and for $T_n > 20$ MeV, the prediction (obtained at a threshold of 3 8 MeV eq. el. en.) is lower than the experimental points, which is most pleasing, since there are indications[15]) that the measured efficiency is too high by ~10% in that energy range.

Fig. 4. Comparison of efficiency measurements with the Monte Carlo predictions for neutron counters between 20 and 150 mm thick: (a) McNaughton et al.[15]), (b) Riddle et al.[16]), (c) Hunt et al.[12]), (d) Leleux et al.[14]).

The Monte Carlo prediction is also in good agreement with the data of Riddle et al.[16]) (fig. 4 b), except for the two highest threshold values for $40 < T_n < 60$ MeV, where it is lower by $\lesssim 20\%$ When extracting the experimental data from fig. 3 of ref. 16, we also noticed at the lowest threshold value an obvious error of the efficiency scale, which we corrected for by applying to the data a constant shift in efficiency of 0.02. A discrepancy of $\lesssim 15\%$ is visible between the prediction and the data of Hunt et al.[12]) (fig 4c) at the lowest threshold value for $T_n > 25$ MeV, whereas the experimental efficiencies at the other thresholds are well reproduced. Furthermore, the data do not show the expected rise at 30 MeV as visible in the efficiency of thicker counters at similar thresholds (around 1.0 MeV eq. el. en.), c.f. the data of Wiegand et al.[5]) presented in fig 3a, Brady et al [8]) in fig 3c, Edelstein et al.[13]) in fig. 3d, and McNaughton et al.[15]) in fig. 4a. The data of Leleux et al.[14]) have also been compared with the Monte Carlo prediction (fig. 4d), obtained at a threshold of 100 keV eq el en., as used by the same authors[14]) in their comparison with other computational methods The data are fairly well reproduced with a maximum disagreement of $\sim 10\%$.

Finally fig 5 shows the very good consistency between the very high threshold (37 MeV eq. el. en.) data of Bollini et al [10]) and the predicted efficiency, computed for the real geometry of the modular counter.

Generally the agreement between the experimental and Monte Carlo efficiencies is quite good and certainly much better than 10% overall; small discrepancies ($10 \div 15\%$) are noticeable in some comparisons with measurements at high threshold (>4 MeV eq. el. en.) for $40 < T_n < 90$ MeV (c.f. also fig. 3 of ref. 111), where the treatment of n–C inelastic channels is more crucial. A small disagreement is also visible in the comparison with the data of Hunt et al.[12]) at the lowest threshold (upper curve in fig. 4c) and Leleux et al [14]) (fig. 4d), but these are in the opposite sense. Both these two counters are ≤ 50 mm thick, and the exact knowledge of the overall light output of the counter becomes more relevant to the correct simulation. Nevertheless in all the comparisons the experimental data in the energy region immediately above the threshold and for energies greater than 100 MeV (also at very high threshold, c.f figs 3c and 5 and fig 3 of ref 111) are always beautifully reproduced.

The computational methods of Kurz[1–2]) and Stanton[3]) have been previously used by several authors[7–16]) for comparison with their own data. We notice that our Monte Carlo results give much better agreement than Kurz's predictions for most of the experiments, especially for the data of McNaughton et al.[15]), Riddle et al.[16]), Leleux et al.[14]) and Bollini et al.[10]) (see figs. 4a, 4b, 4d and 5). We also think that our predictions are better than Stanton's for some experiments, especially for the data of Young et al [9]), McNaughton et al.[15]) and Leleux et al.[14]) (see figs. 3c, 4a and 4d), and show at least the same agreement to within 5% as quoted by Stanton[3]) and illustrated in figs. 3a–d of ref 13, for the data of Crabb et al.[7]), Brady et al.[8]), Edelstein et al.[13]) and Hunt et al [12]) (see figs. 3b, 3c, 3d and 4c).

Finally we would like to stress that in our Monte Carlo program the cross sections shown in figs. 1 and 2 were used, obtained directly from the experimental data, without any 'tuning' as Stanton did[3]). This proved to be very successful in the end, although a better knowledge of each individual n–C inelastic channel would be desirable for obtaining a complete consistency between Monte Carlo and experimental efficiencies.

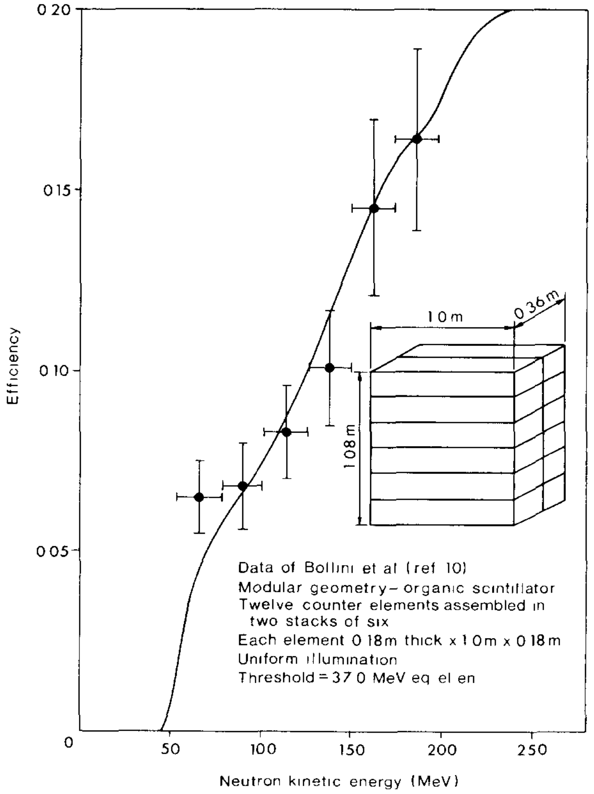

Fig. 5. Comparison of efficiency measurement with the Monte Carlo prediction for a modular counter at a very high threshold[10])

It is a pleasure to thank the Director of the Daresbury Laboratory for his kind hospitality, A. Stefanini for his encouragement and D Clarke for useful comments and suggestions

Note added in proof

Since this paper was originally published as a Daresbury Laboratory Preprint (DL/P245, October 1975), other data have become available in the literature on neutron-proton elastic scattering from 58 to 391 MeV 117) and on ^{11}C total production cross section in n^{12}C interactions between 1 and 2 GeV/c 118)

Furthermore McNaughton et al 119) have recently performed a measurement of ^{12}C(n,p) and ^{12}C(n,d) reactions at 56 MeV, and they have used this result to operate a critical appraisal of the n–C inelastic cross sections (in particular the (n,p) and the (n,n′3α) channels) used in the Stanton's3) and Kurtz's1) code to predict neutron counter efficiencies It is very rewarding to notice that the new experimental points lie very close to the extrapolated cross sections presented here (see fig 2) McNaughton et al also reach much the same conclusions on the other n–C inelastic channels (n,α) and (n,n′γ) as those of fig 2 The fact that very close cross sections, used in different Monte Carlo programs, give predictions in agreement between themselves and with the experimentally measured efficiencies, give us confidence on the adequate treatment of the n—C inelastic channels provided in this paper

References

1) R J Kurz, UCRL-11339 (March 1964), S A Elbakr, J W Watson and C A Miller, Nucl. Instr. and Meth **115** (1974) 115
2) S T Thornton and J R Smith, Nucl. Instr and Meth **96** (1971) 551
3) N R Stanton, COO-1545-92 (February 1971)
4) D Hermsdorf, K Pasieka and D Seeliger, Nucl Instr and Meth **107** (1973) 259
5) C. E Wiegand, T Elioff, W B Johnson, L. B Auerbach, J Lach and Th Ypsilantis, Rev Sci Instr **33** (1962) 526
6) P H Bowen, G C Cox, G B Huxtable, A Langsford, J P Scanlon, G H Stafford and J J Thresher, Nucl Instr and Meth **17** (1962) 117
7) D G Crabb, J G McEwen, E G Auld and A. Langsford, Nucl Instr and Meth. **48** (1967) 87
8) F P. Brady, J A Jungermann, J C Young, J L Romero and P J Symonds, Nucl Instr and Meth **58** (1968) 57, Errata, Nucl Instr and Meth **63** (1968) 358
9) J C Young, J L Romero, F P Brady and J R Morales, Nucl Instr and Meth **68** (1969) 333
10) D Bollini, A Buhler-Broglin, P Dalpiaz, T Massam F. Navach, F L Navarria, M A Schneegans, F Zetti and A Zichichi, Nuovo Cimento **61A** (1969) 125
11) A S L. Parsons, P Truoel, P A Berardo, R P. Haddock, L Verhey and M E Zeller, Nucl Instr and Meth **79** (1970) 43
12) J. B Hunt, C A Baker, C J Batty, P Ford, E Friedman and L. E Williams, Nucl Instr and Meth **85** (1970) 269
13) R M Edelstein, J S Russ, R C. Thatcher, M Elfield, E L Miller, N W Reay, N R Stanton, M A Abolins, M T Lin, K W Edwards and D R Gill, Nucl Instr and Meth **100** (1972) 355
14) P Leleux, P C Macq, J P Meulders and C Pirart, Nucl Instr and Meth **116** (1974) 41.
15) M W McNaughton, F P Brady, W B Broste, A L Sagle and S W Johnsen, Nucl Instr and Meth **116** (1974) 25
16) R A J Riddle, G H Harrison, P G Roos and M J Saltmarsh, Nucl Instr and Meth **121** (1974) 445
17) D. A Kellogg, Phys. Rev **90** (1953) 224
18) H C Evans and E H Bellamy, Proc Roy Soc **74** (1959) 483
19) T J Gooding and H G Pugh, Nucl Instr and Meth **7** (1960) 189
20) D L. Smith, R G Polk and T G Miller, Nucl Instr and Meth. **64** (1968) 157
21) R L Craun and D L Smith, Nucl Instr and Meth **80** (1970) 239
22) W N Hess, Rev. Mod. Phys **30** (1958) 368
23) D J Hughes and R B Schwartz, BNL-325 (July 1958)
24) J R Stehn, M D Goldberg, B A Magurno and R Wiener-Cashman, BNL-325, vol 1, 2nd ed . Suppl 2 (May 1964)
25) V S Barashenkov, K K Gudima and V. D Toneev, Fortschr Physik **17** (1969) 683
26) M Ageno, E Amaldi, D Bocciarelli and G C. Trabacchi, Phys Rev. **71** (1947) 20
27) R A Al-Kital and R A Peck, Jr , Phys Rev **130** (1963) 1500
28) J D Anderson, C C Gardner, J W McClure, M P Nakada and C. Wong, Phys Rev **111** (1958) 572
29) A Ashmore, R G Jarvis, D S Mather and S K Sen, Proc Phys Soc **A70** (1957) 735
30) A Ashmore, R G Jarvis, D S Mather and S K Sen, Proc Phys Soc **A70** (1957) 745
31) A Ashmore, D S Mather and S. K Sen, Proc Phys Soc **A71** (1957) 552
32) J H Atkinson, W N Hess, V Perez-Mendez and R Wallace, Phys Rev **123** (1961) 1850
33) W P Ball, Thesis, UCRL-1938 (August 1952)
34) M E Battat and E R Graves, Phys Rev **97** (1955) 1266
35) J Benveniste, A C Mitchell, C D Schrader and J H Zenger, Nucl Phys **19** (1960) 448
36) N A Bostrom, I L Morgan, J T Prud'homme, P L Okhuysen and O M Hudson, WADC-TN-59-107 (1959)
37) N E Booth, G W Hutchinson and B Ledley, Proc Phys Soc **A71** (1958) 293
38) P. H Bowen J P Scanlon G H. Stafford, J J Thresher and P E Hodgson, Nucl Phys **22** (1961) 640
39) M Auman, F P Brady, J A Jungerman, W J Knox, M R McGie and T C Montgomery, Phys Rev **C5** (1972) 1
40) S G Carpenter and R Wilson, Phys Rev **114** (1959) 510
41) L J. Cook, E M McMillan, J M Petersen and D C Sewell, Phys Rev **75** (1949) 7
42) J H Coon R W Davis, H E Felthauser and D B Nicodemus, Phys Rev **111** (1958) 250
43) T Coor, D A Hill, W F Hornyak, L W Smith and G Snow, Phys Rev **98** (1955) 1369
44) V Culler and R W Waniek Phys. Rev **95** (1954) 585
45) V Culler and R W Waniek, Phys Rev **99** (1955) 740
46) E A Davis, T W Bonner, D W Worley, Jr and R Bass Bull Am Phys. Soc **8** (1963) 115
47) R B Day, Phys Rev **102** (1956) 767
48) R B Day and R L Henkel, Phys Rev **92** (1953) 358
49) R B Day, R L Mills, J E Perry, Jr and F Scherb, Phys Rev **98** (1955) 279

50) T J Devlin, W Johnson, J Norem, K Vosburgh, R E Mischke and W Schimmerling, Phys Rev **D8** (1973) 136

51) J DeJuren, Phys Rev. **80** (1950) 27

52) J DeJuren and N Knable, Phys Rev **77** (1950) 606

53) J DeJuren and B. J. Moyer, Phys Rev. **81** (1951) 919

54) W M Deuchars and D Dandy, Proc Phys Soc **75** (1960) 855

55) V P Dzhelepov, V I Satarov and B M Golovin, in Report of Institute of Nuclear Physics, Moscow, (1952)

56) V P Dzhelepov, V I Satarov and B M Golovin, Zh Eksper Teor Fiz **29** (1955) 369

57) V P Dzhelepov, V I Satarov and B M Golovin, Dokl. Akad Nauk SSSR **104** (1955) 717

58) R Fox, C Leith, L Wouters and K R. MacKenzie, Phys Rev **80** (1950) 23

59) G M Frye, Jr , L. Rosen and L Stewart, Phys Rev. **99** (1955) 1375

60) E. Haddad and D D Phillips, Bull Am Phys Soc **4** (1959) 358

61) J Hadley, E. L Kelly, C E Leith, E Segrè, C Wiegand and H F York, Phys Rev **75** (1949) 351.

62) P Hillman, R. H Stahl and N F Ramsey, Phys Rev. **96** (1954) 115

63) R. H Hildebrand and C E Leith, Phys Rev **80** (1950) 842

64) Yu M Kazarinov, V. I Satarov and Yu K Simonov, Yader Fiz **1** (1965) 271

65) H Kitazawa and N Yamamuro, J Phys Soc Jap **26** (1969) 600

66) W E Kreger and B. D Kern, Phys Rev **113** (1959) 890

67) A H Lasday, Phys Rev **81** (1951) 139

68) W I Linlor, UCRL-2303 (1953)

69) M H MacGregor, W P Ball and R Booth, Phys Rev **111** (1958) 1155

70) G R Mott, G L Guernsey and B K Nelson, Phys Rev **88** (1952) 9

71) D F Measday and J N Palmieri, Nucl Phys **85** (1966) 129

72) V Meyer, R M Eisberg and R F Carlson, Phys Rev **117** (1960) 1334

73) D I Meyer and W Nyer, LA-1279 (July 1951)

74) M P. Nakada, J D Anderson, C C Gardner and C Wong, Phys Rev **110** (1958) 1439.

75) V A Nedzel. Phys. Rev **94** (1954) 174

76) V S Pantuyev and M H Khachaturyan, Zh. Eksper Teor Fiz **42** (1962) 909

77) R W Peelle, Phys Rev **105** (1957) 1311

78) H L Poss, E O Salant, G A Snow and L C L Yuan, Phys Rev **87** (1952) 11

79) E O Salant and N F Ramsey, Phys Rev **57** (1940) 1075

80) V E. Scherrer, R B Theus and W R Faust, Phys Rev. **91** (1953) 1476

81) W Schimmerling, Th J Devlin, W W Johnson, K G Vosburgh and R E Minschke, Phys Rev **C7** (1973) 248

82) W Schimmerling, Th. J Devlin, W W Johnson, K G Vosburgh and R E Minschke, Phys Lett **37B** (1971) 177

83) R Sherr, Phys. Rev **68** (1945) 240

84) J B Singletary and D E Wood, Phys Rev. **114** (1959) 1595.

85) W Sleator, Jr., Phys Rev **72** (1947) 207

86) K. Strauch and F. Titus, Phys. Rev **103** (1956) 200.

87) A E Taylor, Phys. Rev. **92** (1953) 1071.

88) A E Taylor, T G. Pickavance, J M. Cassels and T. C Randle, Phil. Mag. **42** (1951) 328.

89) A E Taylor, T G Pickavance, J M Cassels and T. C Randle, Phil Mag **42** (1951) 571

90) A E Taylor and E Wood, Phil Mag **44** (1953) 95.

91) K Tesch, Nucl Phys **37** (1962) 412

92) L C Thompson and J. R Risser, Phys. Rev **94** (1954) 941

93) H Tyren and Th A J. Maris, Nucl Phys **4** (1957) 637

94) C P Van Zyl, R G P Voss and R Wilson, Phil Mag **1** (1956) 1003

95) R G. P Voss and R Wilson, Proc Roy Soc **A236** (1956) 41

96) M Walt and J R Beyster, Phys Rev **98** (1955) 677

97) S J Bame, Jr , E Haddad, J E Perry, Jr and R K Smith, Rev. Sci Instr **28** (1957) 997

98) *Fast Neutron Physics* (eds. J B Marion and J L Fowler, Interscience, New York, 1963) part 2, p. 2209

99) Th P Clements and L Winsberg, UCRL-9043 (February 1960)

100) The dependence of the neutron-nucleus cross sections on the atomic weight of the target can be approximated (see ref 81), in the range $350 < T_n$ 1800 MeV, by a A^β law, where β varies very little with T_n, from 0 72 to 0 84, at higher energies (see refs 102, 103), between 6 and 19 GeV the neutron–nucleus cross sections have a T_n dependence even more similar to the n–p total cross sections Indeed, if they are normalized to σ_{np}, no T_n dependence can be observed

101) CERN computer Program Library, Program MINUIT

102) J Engler, K Horn, J Konig, F Monnig, P Schludecker, H. Schopper, P Sievers, H Ullrich and K Runge, Phys Lett. **28B** (1968) 64

103) J Engler, K. Horn, F Monnig, P Schludecker, W Schmidt-Parzefall, H Schopper, P Sievers, H Ullrich, R Hartung, K Runge and Yu Galaktionov, Phys Lett **32B** (1970) 716

104) S Pearlstein Nucl Data, Sect A **3** (1967) 327

105) For a full discussion on energy levels of carbon, see F. Ajzenberg-Selove and T Lauritsen, Nucl Phys **11** (1959) 1

106) G A Grin, B Vaucher, J C Alder and C Joseph, Helv Phys Acta **42** (1969) 990.

107) J F Loude, J. P Perroud and Ch Sellem, Helv Phys Acta **42** (1969) 905

108) J. F Loude, J P Perroud and Ch Sellem, Helv Phys Acta **44** (1970) 33

109) G Betti, Thesis (University of Pisa, 1972) unpublished

110) A Del Guerra, M A Giorgi, A Giazotto, A Stefanini, D W Braben and D Clarke, Daresbury Laboratory Internal Report DNPL/TM75 (November 1970) unpublished

111) G Betti, A Del Guerra, A Giazotto, M A Giorgi, A Stefanini, D R Botterill, D W Braben, D Clarke and P R. Norton, Nucl Instr and Meth **135** (1976) 319

112) G Betti, D R Botterill, D W Braben, D Clarke, A Del Guerra, A Giazotto, M A Giorgi, P R Norton and A Stefanini, Proc Int Conf on *Instrumentation for high energy physics*, Frascati May 1973 (ed. S Stipcich, CNEN, Frascati, 1973) p 422

113) A Del Guerra, A Giazotto, M A Giorgi, A Stefanini, D R. Botterill, D W Braben, D Clarke and P R Norton, Nucl Instr and Meth **135** (1976) 307

114) J. Bailey, D. R Botterill, D Clarke, H E. Montgomery, P R. Norton, G Matone, A Del Guerra, A. Giazotto M. A. Giorgi and A Stefanini, Nucl. Instr and Meth **135** (1976) 331

115) J W Watson and R G Graves, Nucl Instr and Meth. **117** (1974) 541

116) R De Leo, G. D'Erasmo, A Pantaleo and G Russo, Nucl Instr and Meth **119** (1974) 559

[117]) A. J. Bersbach, R. E. Mischke and T J Devlin, Phys Rev **13D** (1976) 535.

[118]) G Bizard, F. Bonthonneau, J.L. Laville, F. Lefebvres, J C. Malherbe, R. Regimbart, J. Duflo, F. Plouin and H Quechon, Nucl Instr and Meth **129** (1975) 569

[119]) M W McNaughton, N S P King, F P Brady and J L Ullmann, Nucl Instr. and Meth **129** (1975) 241